International Journal of Chinese Medicine
2022; 6(2): 20-33
http://www.sciencepublishinggroup.com/j/ijcm
doi: 10.11648/j.ijcm.20220602.11
ISSN: 2578-9465 (Print); ISSN: 2578-9473 (Online)

Fine Analysis of the Binding Mode Between Traditional Chinese Chemical Components and 2019-nCoV RNA Polymerase Based on Molecular Docking Technology

Ji-chao Wei[1], Qian Liu[2, *], Yan-Lei Su[3, *], An-Tang Peng[4], Xu-Hong Duan[5]

[1]Department of Pharmacy, The Third Hospital of Hebei Medical University, Shijiazhuang, China

[2]Department of Geriatrics, Youfu Hospital, Shijiazhuang, China

[3]Department of Pharmacy, The 980th Hospital of the Logistics Support Force of the Chinese People's Liberation Army, Shijiazhuang, China

[4]Department of Pharmacy, The Traditional Chinese Medicine Hospital of Shijiazhuang, Shijiazhuang, China

[5]Traditional Chinese Medicine Processing Technology Innovation Center of Hebei Province, Hebei University of Chinese Medicine, Shijiazhuang, China

Email address:

1010846442@qq.com (Qian Liu), suyanlei0161@163.com (Yan-Lei Su)

[*]Corresponding author

To cite this article:

Ji-chao Wei, Qian Liu, Yan-Lei Su, An-Tang Peng, Xu-Hong Duan. Fine Analysis of the Binding Mode Between Traditional Chinese Chemical Components and 2019-nCoV RNA Polymerase Based on Molecular Docking Technology. *International Journal of Chinese Medicine*. Vol. 6, No. 2, 2022, pp. 20-33. doi: 10.11648/j.ijcm.20220602.11

Received: May 28, 2022; **Accepted**: July 5, 2022; **Published**: July 20, 2022

Abstract: Sing SARS RNA polymerase 6NUR as a template, a three-dimensional structural model of the novel coronavirus' RNA polymerase was constructed with a homology modeling approach. It was used as an antiviral research target and refined to analyze the molecular interaction between amino acid and substrate inhibitors in target enzyme NTPs binding sites. The virtual screening showed that flavonoids are novel coronavirus resistant active ingredients. The results of the study proved to be highly relevant to antiviral clinical practice and consistent with the fact that some flavonoids are NS5B inhibitors and thus have anti-HCV activity. We hope that our report will attract the attention of researchers at home and abroad, and through further experimental validation, it will help us to develop better anti-novel coronavirus drugs as soon as possible.

Keywords: 2019-Novel Coronavirus, Traditional Chinese Medicine, RNA Polymerase, Homology Modeling, 6NUR, 6M71, Molecular Docking, Inhibitors, Remdesivir, Favipiravir, Flavonoid, Hepatitis C virus, NS5B

1. Introduction

In early February, the author constructed a three-dimensional structural model of a novel coronavirus RNA polymerase using SARS-RNA polymerase 6NUR as template, which was used to verify the interaction between the target enzyme molecule and chemical components derived from the constitutive relationship [1]. Based on the results of the study, the author inferred that (1) In China, Remdesivir may not be needed to fight the novel coronavirus epidemic. This is not to deny the antiviral activity of Remdesivir against the novel coronavirus, on the contrary we believe that it's a useful drug, but we found that there are many compounds with the same mechanism as Remdesivir and similar binding strength with the target enzyme (for example, some flavonoid natural products with good safety widely exist in vegetables, fruits and some traditional Chinese medicines). We speculate that these compounds also have good inhibitory activity of novel coronavirus RNA polymerase and may cure novel coronavirus infection without using Remdesivir. (2) The commonly used clinical traditional Chinese medicine ephedra, Astragalus membranaceus, Belamcanda, Fructus Trichosanthis, Agastache, Agastache ragosus, ginger etc. all contain flavonoids. The use of traditional Chinese medicine formula decoction can make the antiviral chemical components (such as flavonoids) add up to a certain amount and play the role of antiviral treatment. The lung clearing and detoxification decoction as a representative of a variety of Chinese medicine prescription will be an effective drug for novel coronavirus infected patients in

China. The clinical practice of China's fight against the epidemic has proved that the author's conclusion is correct, and the research results are of scientific and reference value.

Several groups of scholars at home and abroad have adopted similar research methods [2-7]: using homology modeling to study the interaction between inhibitor and novel coronavirus RNA polymerase, but their research results are not exactly the same. The results of the author's study are close to those of Muhammad, Ashleigh and later crystal structure analysis [8-11]. There may be many cavities that can bind to small molecules in the three-dimensional structure of any large protein molecule, but not all small molecules that can bind to protein cavities will have corresponding biological activities in nature. In this report, the binding effect of 27 compounds mainly composed of traditional Chinese medicine chemical components and the novel coronavirus RNA polymerase model in the three-dimensional space was explained, and the possible correct binding modes of these compounds at the target enzyme activity site were analyzed and reasoned, providing reference for the development of anti-novel coronavirus and clinical treatment.

2. Theoretical Derivation of Structure-Activity Relationship

The novel coronavirus invades the cells and reproduces itself to form a large number of progeny virus monomers. Blocking a certain link in the life cycle of a virus can make its life system stay in a relatively static state, and many of its life elements can be exposed to the host cell biochemical reaction system, such as proteasome, endonuclease RNaseA and L19RNA, which can destroy the key life elements of the virus life system, so that the substances of the virus life system are ultimately eliminated, transformed and utilized by the cells system. The papain-like protease of SARS also has the activity of deaubiquitinase (DUB), which can block the ubiquitination pathway of related proteins. The maintenance of RNA virus's life cycle can't bypass the central information transmission link of RNA synthesis. The nucleoside inhibitors, such as Remdesivir, Favipiravir, Sofosbuvir, Ribavirin, all act on the key target of RNA polymerase to block RNA synthesis, and finally achieve the effective antiviral purpose.

According to the description of the initial symptoms of infection in patients with novel coronavirus (low fever, fatigue, cough, etc.), the author thinks that it possibly belongs to the category of "cold syndrome" of traditional Chinese medicine. Therefore, the chemical components of traditional Chinese medicine that dispel pathogenic cold and relieve exterior syndrome (mainly ginger and ephedra) are taken as the important research objects to excavate antiviral components. The essence of drug action is the proper interaction between small molecules of a compound and biomolecules. Flavonoids are a class of compounds abundant in these herbal medicines, and we found that the 1, 2, 3 and 4 positions in the RNA polymerase substrate guanine nucleoside structure can overlap with the 1, 2, 3 and 4 positions in flavonoids, and the six-membered sugar ring part of flavone-7-glucoside can occupy the five-membered sugar ring position region at the target enzyme active site and can form intermolecular interactions, see Figure 1 for chemical structure. Accordingly, it is speculated that certain flavonoids may be novel coronavirus RNA polymerase inhibitors, and we further used molecular docking technology to study the binding pattern of relevant compounds and enzyme activity sites.

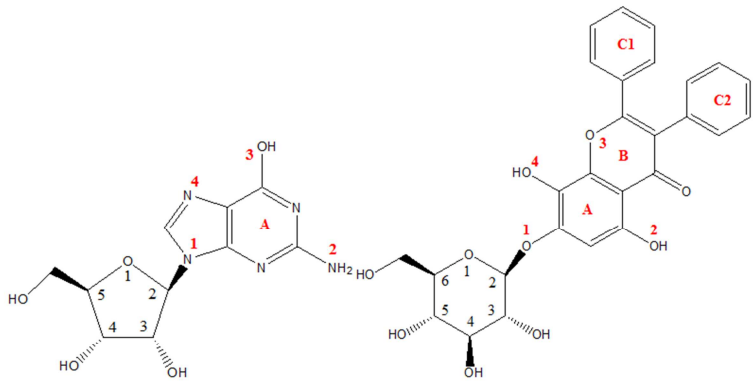

Guanosine Flavonoids -7-O-glucose (flavonoid glycosides)

Figure 1. *Structure of guanosine and flavonoids -7-O-glucose.*

3. Molecular Docking Experiment Process

3.1. Molecular Modeling of Target Proteins

The novel coronavirus RNA polymerase amino acid sequence was submitted to Swiss-Model Server for homology modeling, and the homology similarity between the amino acid sequence and the RNA polymerase structure 6NUR of SARS was 96%. The coverage rate was very high and reached the requirements of modeling standards, so a 3d structure model of 2019-nCoV-RNA polymerase was constructed using 6NUR as a template. As shown in Figure

2A, amino acids 1-116 at N-terminal, which are disordered in spatial structure and far away from the active center of the target enzyme, are deleted in the model, and the structure of 2019-nCoV polymerase model and SARS polymerase is overlapped (see Figure 2B, 3D structure of SARS polymerase 6NUR shown in blue). After the novel coronavirus RNA polymerase 3D structure 6M71 was published, the author superimposed the model structure with it, RMS value is 1.335 (see Figure 2C, 6M71 shown in green, the model structure shown in red).

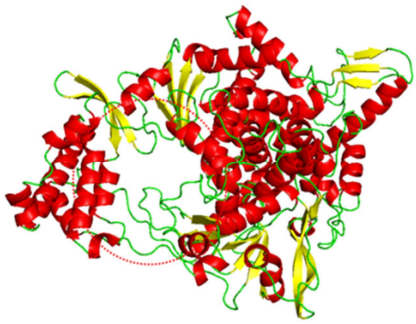

A: 3D structure of 2019ncov RNA polymerase

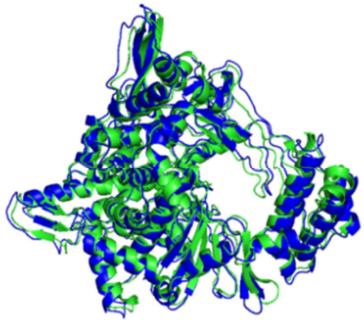

B: structure superposition of construction model and SARS virus RNA polymerase

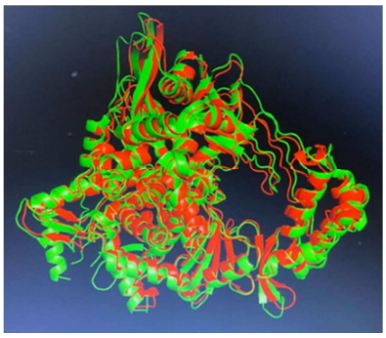

C: construction model overlapped with the structure of 6M71

Figure 2. *Structure of RNA polymerase.*

The three-dimensional structure of the obtained model protein is mainly composed of more than 30 α helices, 18 β folds and random curls. Its active sites are mainly composed of helices and random curls. The hydrophobic groove of the protein is located on the inner surface of the protein. After nucleotides (NTPs) enter the region [12], ribose 2 '-OH can form hydrogen bond interaction with Thr564 (Thr680 on 6NUR) and Asn575 (Asn691 on Asn691), and 3'-OH can form hydrogen bond interaction with Asp507 (Asp623 on 6NUR). Furthermore, Val441 (Val557 on SARS) also affects the base pairing of NTPs with the template RNA after entering the active site. If small molecule ligands and NTPs act on this active site by means of competition, they can antagonize the replication process of 2019-nCoV-RNA.

3.2. Selection of Small Molecular Ligands

Referring to the chemical components of ephedra, ginger and other Traditional Chinese medicines as well as influenza virus RNA polymerase inhibitors, the author set some target compounds for molecular docking research with the target model. The structures of these compounds are shown in Figure 3 below.

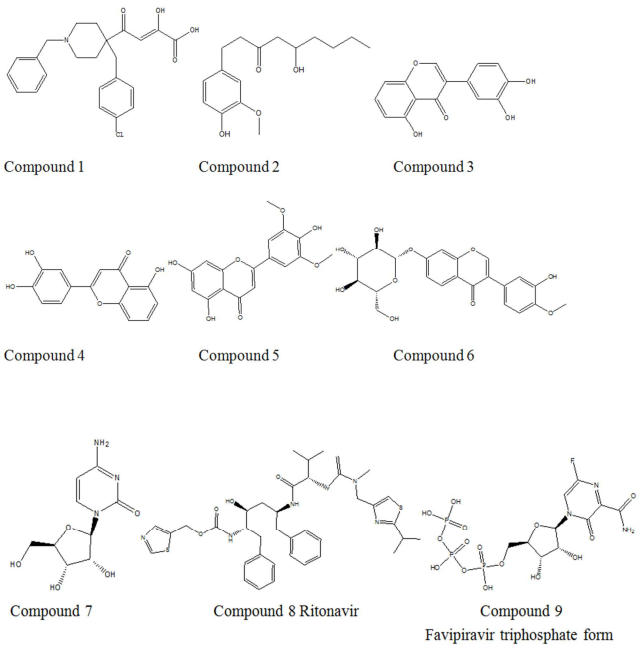

Compound 1 Compound 2 Compound 3

Compound 4 Compound 5 Compound 6

Compound 7 Compound 8 Ritonavir Compound 9 Favipiravir triphosphate form

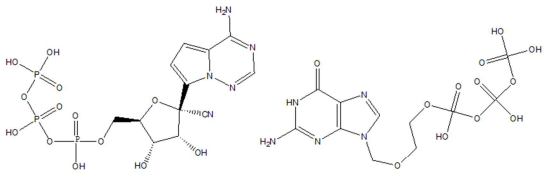

Compound 10 Remdesivir triphosphate form

Compound 11 Acyclovir triphosphate form

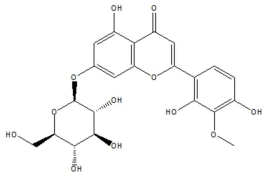

Compound 12

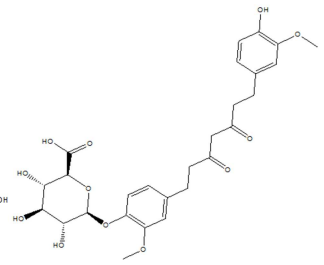

Compound 13 Curcumin metabolite

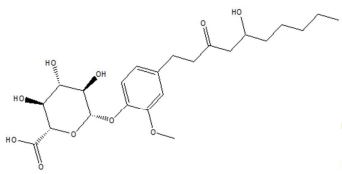

Compound 14 6-gingerol metabolites

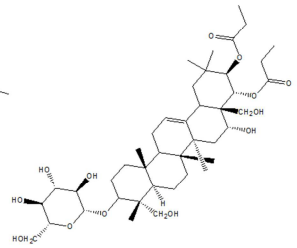

Compound 15

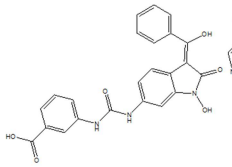

Compound 16

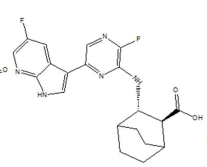

Compound 17

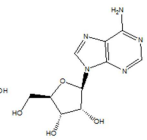

Compound 18 Adenosine

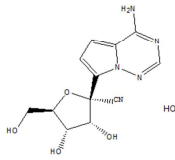

Compound 19

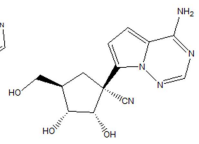

Compound 20

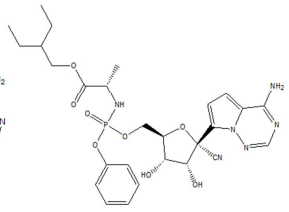

Compound 21 Remdesivir

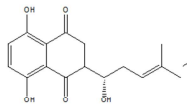

Compound 22 Alkannin

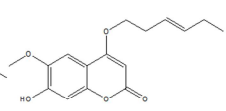

Compound 23

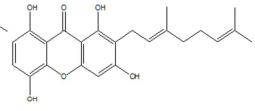

Compound 24

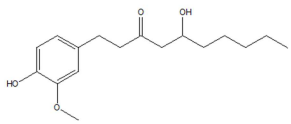

Compound 25

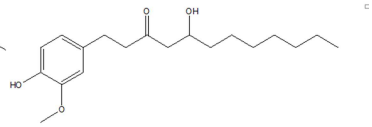

Compound 26

Figure 3. *Structure of the compound.*

3.3. Molecular Docking and Operation Process

3.3.1. Ligand Treatment

We use Chemidraw 14.0 to deal with the structure of small molecules, use MM2 force field to minimize the energy and save it to mo12 format, then use Mgtools 1.5.6 to deal with it, through hydrogenation, calculate the charge and combine the non-polar hydrogen to save it to pdbqt file.

3.3.2. Receptor Treatment

Three-dimensional structure of the protein was obtained from PDB database. Mgtools 1.5.6 was used to deal with the structure of the protein. Pdbqt file was saved after hydrogenation, calculation of charge and incorporation of nonpolar hydrogen.

3.3.3. Use the Molecular Docking Software Autodock Vina for Docking

A 22.5*15*15 box was constructed with the active site of the protein (center x = 145.956, center y = 144.227, center z = 154.397) as the center, which was enough to cover the related active site in the target enzyme structure, and pdbqt file was generated by Vina operation.

3.3.4. Result Processing

The pdbqt file and protein structure were opened with Pymol1.7.2.1 software, pdb files were saved, and the related graphics were processed.

4. Molecular Docking Results

The free energy released by the intermolecular interaction between compound 1-27 and the target enzyme active site is shown in Table 1, in kal /mol.

The molecular docking results of compounds 1-15 are described in Reference 1.

Compound 16 mainly interacts with LYS435, ARG437, VAL441, ASP502, TYR503, CYS506, ASP507, SER566, ALA572, ASP644 and other amino acid residues at the active site of protein. The docking energy is -8.3kal/mol. The ligand interacts with the protein, which mainly forms 5 hydrogen bonds with LYS435, ARG437, CYS506, SER566. The hydrogen bond length is 2.3, 2.6, 2.3, 2.6 and 1.9Å, respectively. The formation of hydrogen bond increases the ability of ligand targeting protein.

Compound 17 mainly interacts with LYS435, ARG437, ARG439, ASP502, TYR503, LYS505, CYS506, ASP507, THR564, ASN575, SER643, ASP644 and other amino acid residues at the active site of protein. The docking energy is -8.3kal/mol. The ligand interacts with the protein, which mainly forms 11 hydrogen bonds with LYS435, ARG439, ARG439, ASP502, TYR503, LYS505, LYS505, CYS506, THR564, ASN575 and ASN575. The hydrogen bond length is 2.9, 2.46, 2.49, 2.38, 2.39, 1.96, 2.70, 2.44, 2.94, 2.55 and 2.89Å, respectively. The formation of hydrogen bond increases the ability of ligand targeting protein.

Compound 18 mainly interacts with ARG439, CYS506, ASP507, THR571, ALA572, ASN575, SER643 and other amino acid residues at the active site of protein. The docking energy is -6.3kal/mol. The ligand interacts with the protein, which mainly forms 5 hydrogen bonds with CYS506, ASP507, ASP507, ALA572 and ASN575. The hydrogen bond length is 2.41, 2.21, 2.60, 2.60 and 2.60Å, respectively. The formation of hydrogen bond increases the ability of ligand targeting protein.

Compound 19 mainly interacts with LYS435, ARG437, ARG439, THR440, ASP502, LYS505, ASP507, SER643, ASP644 and other amino acid residues at the active site of protein. The docking energy is -6.9kal/mol. The ligand interacts with the protein, which mainly forms 4 hydrogen bonds with ARG439, ARG439, ASP502 and SER643. The hydrogen bond length is 2.76, 2.40, 2.22 and 2.80Å, respectively. The formation of hydrogen bond increases the ability of ligand targeting protein.

Compound 20 mainly interacts with ARG437, ARG439, ASP502, TYR503, LYS505, CYS506, ASP507, ARG508, ASP644 and other amino acid residues at the active site of protein. The docking energy is -6.3kal/mol. The ligand interacts with the protein, which mainly forms 6 hydrogen bonds with ARG437, ARG437, ASP502, CYS506, ASP507 and ASP644. The hydrogen bond length is 2.57, 2.91, 2.14, 2.77, 2.26 and 2.63Å, respectively. The formation of hydrogen bond increases the ability of ligand targeting protein.

Compound 21 (Remdesivir) mainly interacts with LYS435, ARG437, ARG439, ASP502, LYS505, CYS506, ASP507, ALA572, ASN575, LEU642, ASP644 and other amino acid residues at the active site of protein. The docking energy is -6.3kal/mol. It acts on protein active site in noncovalent binding mode, which mainly forms 1 hydrogen bond with CYS506. The hydrogen bond length is 2.8Å. The formation of hydrogen bond increases the ability of ligand targeting protein.

Compound 22 (Alkannin) mainly interacts with Lys435, ARG437, ARG439, ASP502, TYR503, LYS505, CYS506, ASP507, THR571, ASN575, ASP644 and other amino acid residues at the active site of protein. The docking energy is -3.1kal/mol. It acts on protein active site in noncovalent binding mode, which mainly forms 3 hydrogen bonds with CYS506, ASP507 and ASN575. The hydrogen bond length is 2.6, 2.3 and 2.1A, respectively. The formation of hydrogen bond increases the ability of ligand targeting protein.

Compound 23 mainly interacts with ARG439, CYS506, ASP507, THR564, ALA572, ASN575, SER643 and other amino acid residues at the active site of protein. The docking energy is -3.1kal/mol. It acts on protein active site in noncovalent binding mode, which mainly forms 2 hydrogen bonds with CYS506 and ASP507. The hydrogen bond length is 2.48 and 2.81Å, respectively. The formation of hydrogen bond increases the ability of ligand targeting protein.

Compound 24 mainly interacts with LYS435, ARG437,

ARG439, ASP502, CYS506, ASP507, SER566, ASN575 and other amino acid residues at the active site of protein. The docking energy is -3.1kal/mol. It acts on protein active site in noncovalent binding mode, which mainly forms 1 hydrogen bond with CYS506. The hydrogen bond length is 2.99Å. The formation of hydrogen bond increases the ability of ligand targeting protein.

Compound 25 mainly interacts with ARG437, ARG439, LYS505, ASP507, ALA572, SER643, ASP644 and other amino acid residues at the active site of protein. The docking energy is -3.1kal/mol. It acts on protein active site in noncovalent binding mode, which mainly forms 2 hydrogen bonds with ARG437 and ASP644. The hydrogen bond length is 2.55 and 2.67Å, respectively. The formation of hydrogen bond increases the ability of ligand targeting protein.

Compound 26 mainly interacts with ARG437, ARG439, LYS505, CYS506, ASP507, ALA572, ASN575, LEU642, SER643, ASP644, ASP645 and other amino acid residues at the active site of protein. The docking energy is -3.1kal/mol. It acts on protein active site in noncovalent binding mode, which mainly forms 3 hydrogen bonds with ARG437, ARG437 and ASP644. The hydrogen bond length is 2.44, 3.02 and 2.54Å, respectively. The formation of hydrogen bond increases the ability of ligand targeting protein.

Compound 27 mainly interacts with ARG437, ARG439, CYS506, ASP507, SER566, THR571, ALA572, ASN575, LEU642, SER643, ASP644 and other amino acid residues at the active site of protein. The docking energy is -3.1kal/mol. It acts on protein active site in noncovalent binding mode, which mainly forms 3 hydrogen bonds with ASP507, ASP507 and SER566. The hydrogen bond length is 2.45, 2.79 and 2.24Å, respectively. The formation of hydrogen bond increases the ability of ligand targeting protein.

In the results of this study, Compounds 1-27 mainly enter the target protein active site through hydrophobic and van der Waals force interactions, and form intermolecular hydrogen bond, hydrophobic and van der Waals force interactions with amino acids at the target enzyme active site in a non-covalent manner, and compete with NTPs to form competitive inhibition at the target enzyme active site. Diagramming with PyMOL, the binding diagram of Compound 5, 7, 9, 10, 11, 16, 17, 18, 19, 20 with target protein model can be divided into 4-1, 4-2, 4-3, 4-4, 4-5, 4-6, 4-7, 4-8, 4-9, 4-10. The two-dimensional plane diagrams of the combination of compounds 3, 4, 6, 9, 10, 12, 13, 14, 16 and 17 with the target protein model are shown in Figures 14-23, respectively; Diagramming with ChemDraw, the spatial conformation of the binding of Compounds 2, 5, 6, 9, 10, and 12 to amino acids at the active site of the target enzyme model is shown in Figures 24-29, respectively, and the spatial conformation of the binding of compounds at the active site of the target enzyme is shown in Figure 30, where the dashed line indicates the hydrogen bond formed and the solid red line indicates the interatomic distance (in Å), and the conformation of the binding of Compound 10 to the active site of the target enzyme is shown in Figure 30.

Table 1. *Free energy unit released by docking between the compound and the target enzyme model molecule: Kal/mol.*

Compound 1	-6.5	Compound 10	-7.9	Compound 19	-6.9
Compound 2	-5.6	Compound 11	-6.9	Compound 20	-6.3
Compound 3	-6.7	Compound 12	-7.5	Compound 21	-6.3
Compound 4	-7.1	Compound 13	-6.6	Compound 22	-6.5
Compound 5	-7.0	Compound 14	-6.9	Compound 23	-5.6
Compound 6	-7.6	Compound 15	-4.2	Compound 24	-6.7
Compound 7	-5.9	Compound 16	-8.3	Compound 25	-5.3
Compound 8	-6.1	Compound 17	-8.3	Compound 26	-5.3
Compound 9	-7.8	Compound 18	-6.3	Compound 27	-6.1

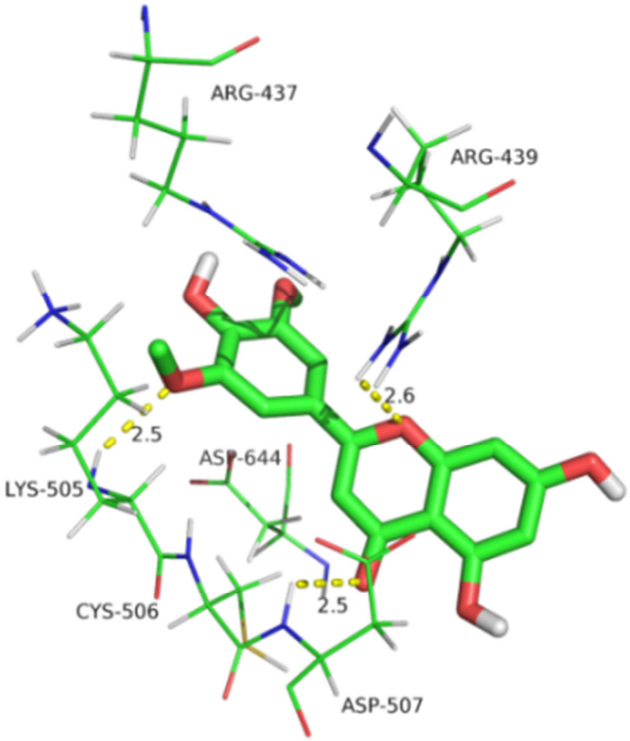

Figure 4. *Binding of Compound 5 to active sites of target enzymes.*

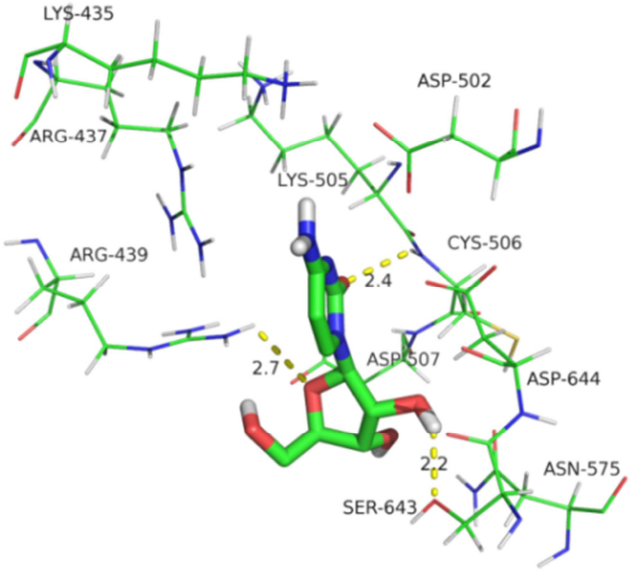

Figure 5. *Binding of Compound 7 to active sites of target enzymes.*

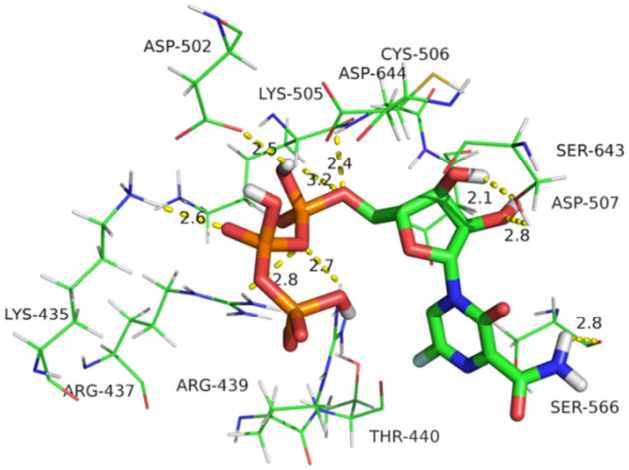

Figure 6. *Binding of Compound 9 to active sites of target enzymes.*

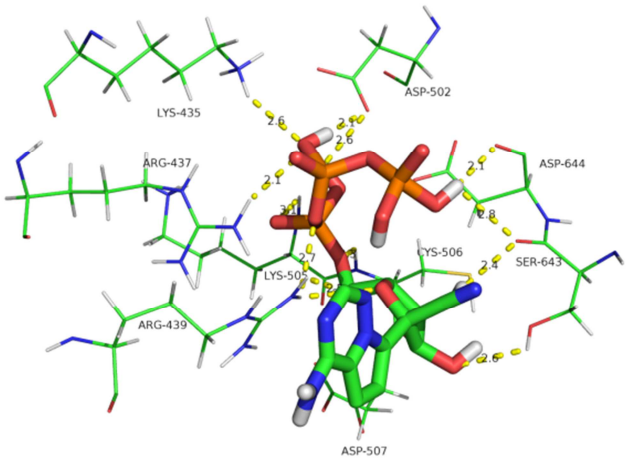

Figure 7. *Binding of Compound 10 to active sites of target enzymes.*

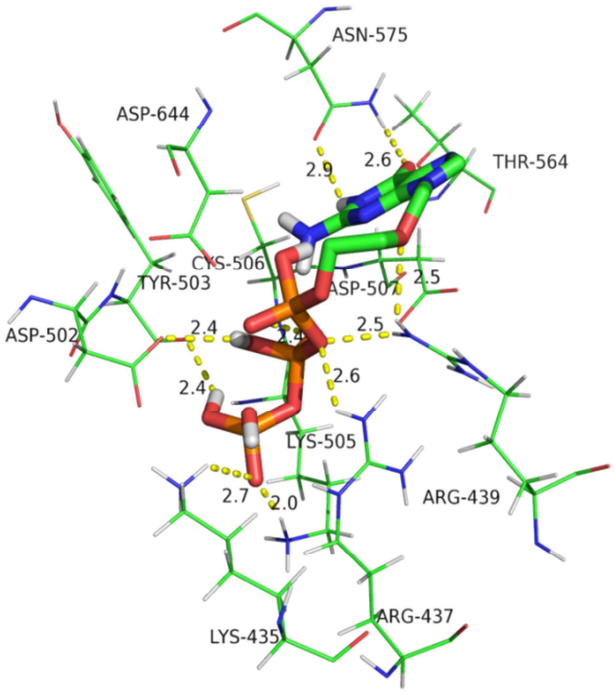

Figure 8. *Binding of Compound 11 to active sites of target enzymes.*

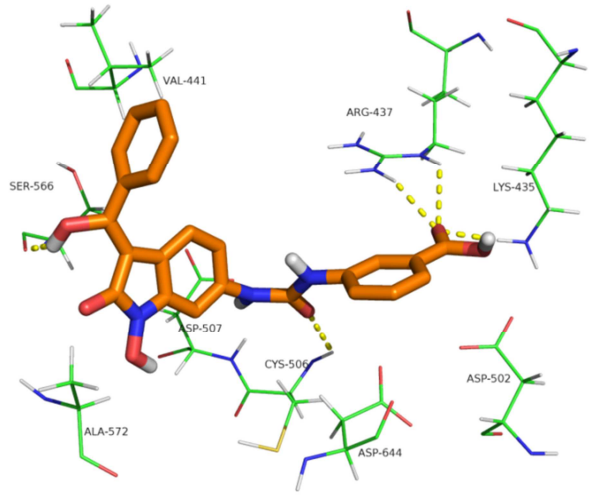

Figure 9. *Binding of Compound 16 to active sites of target enzymes.*

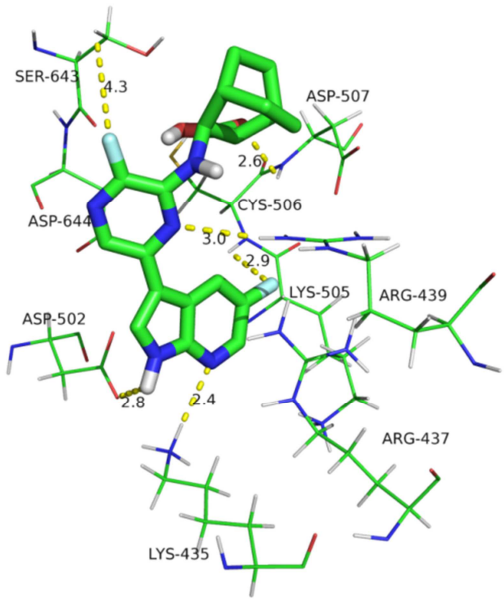

Figure 10. *Binding of Compound 17 to active sites of target enzymes.*

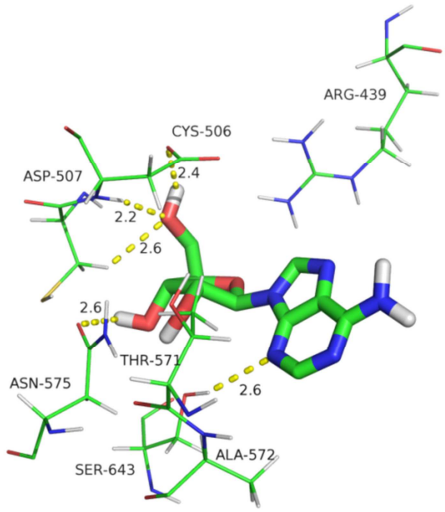

Figure 11. *Binding of Compound 18 to active sites of target enzymes.*

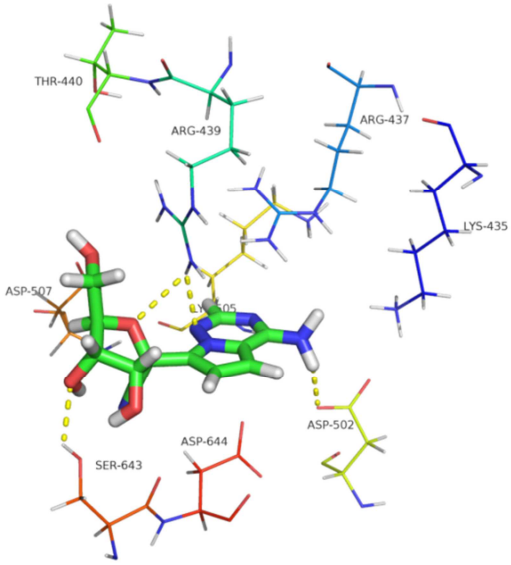

Figure 12. *Binding of Compound 19 to active sites of target enzymes.*

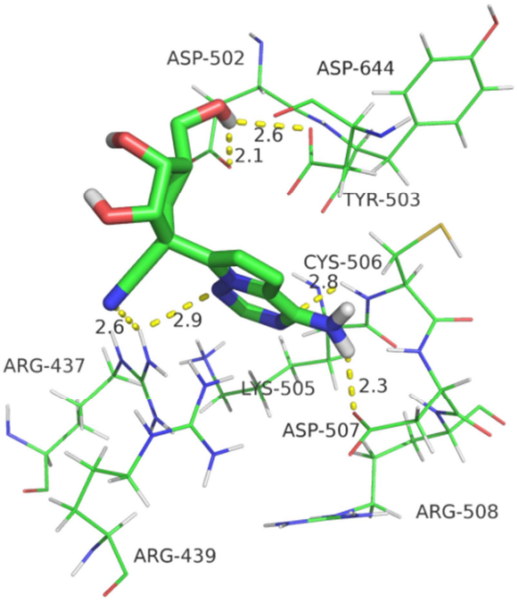

Figure 13. *Binding of Compound 20 to active sites of target enzymes.*

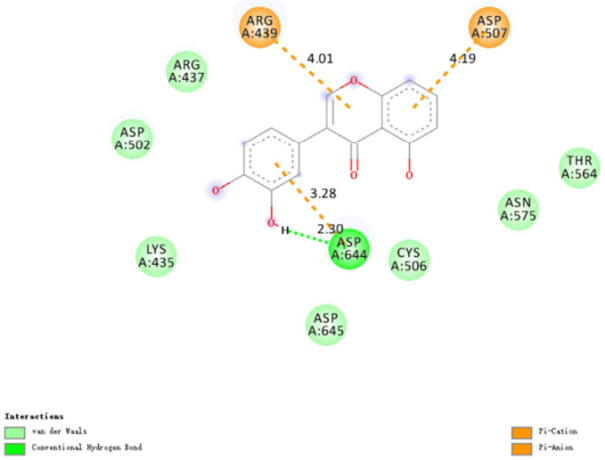

Figure 14. *Binding of Compound 3 to active sites of target enzymes.*

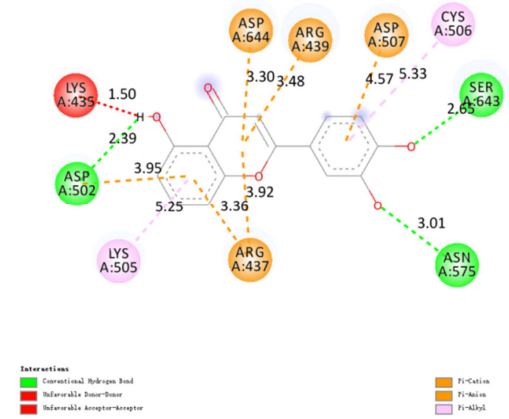

Figure 15. *Binding of Compound 4 to active sites of target enzymes.*

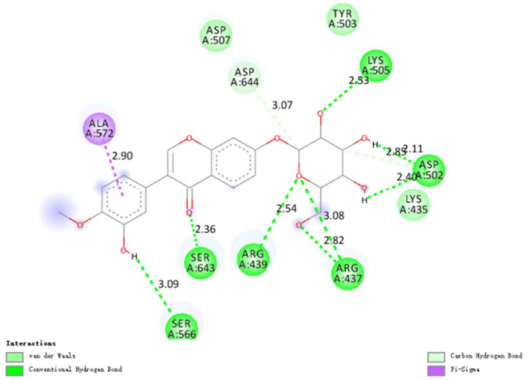

Figure 16. *Binding of Compound 6 to active sites of target enzymes.*

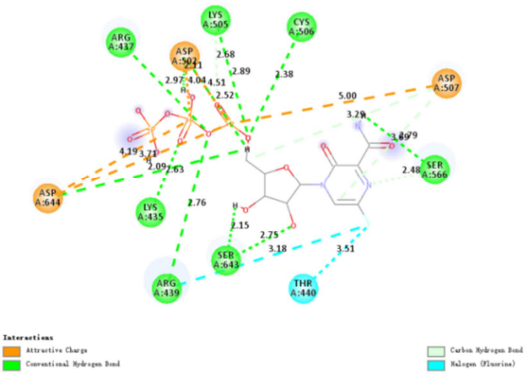

Figure 17. *Binding of Compound 9 to active sites of target enzymes.*

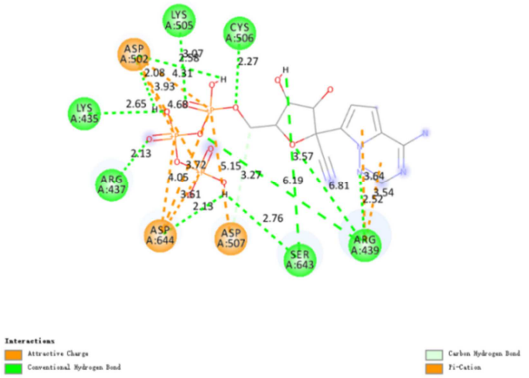

Figure 18. *Binding of Compound 10 to active sites of target enzymes.*

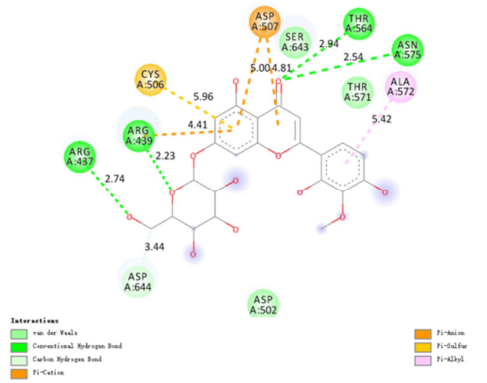

Figure 19. *Binding of Compound 12 to active sites of target enzymes.*

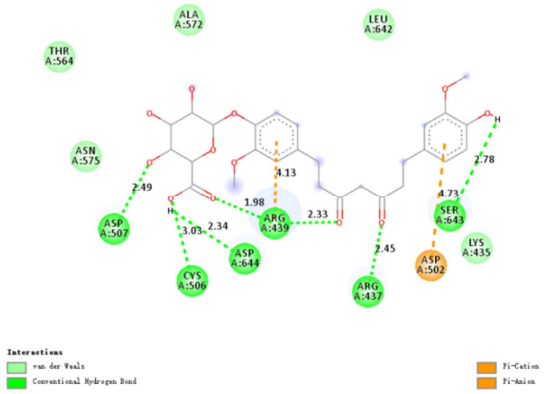

Figure 20. *Binding of Compound 13 to active sites of target enzymes.*

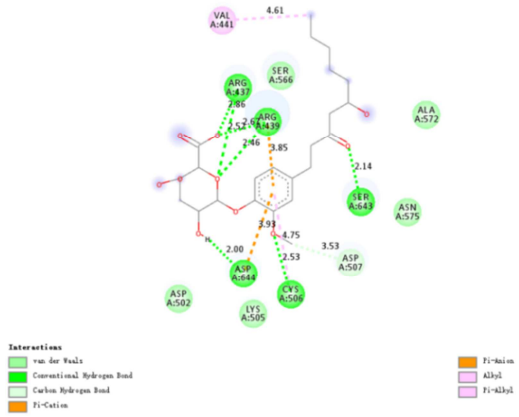

Figure 21. *Binding of Compound 14 to active sites of target enzymes.*

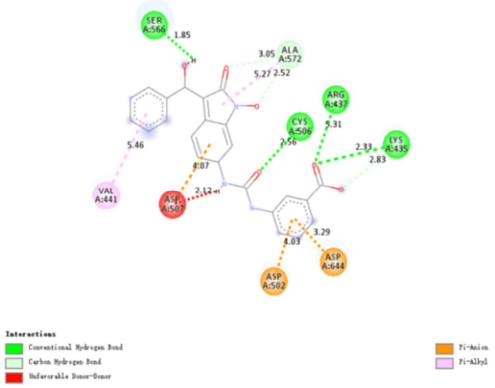

Figure 22. *Binding of Compound 16 to active sites of target enzymes.*

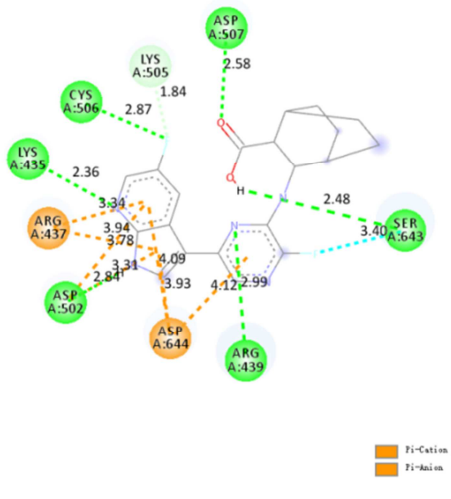

Figure 23. *Binding of Compound 17 to active sites of target enzymes.*

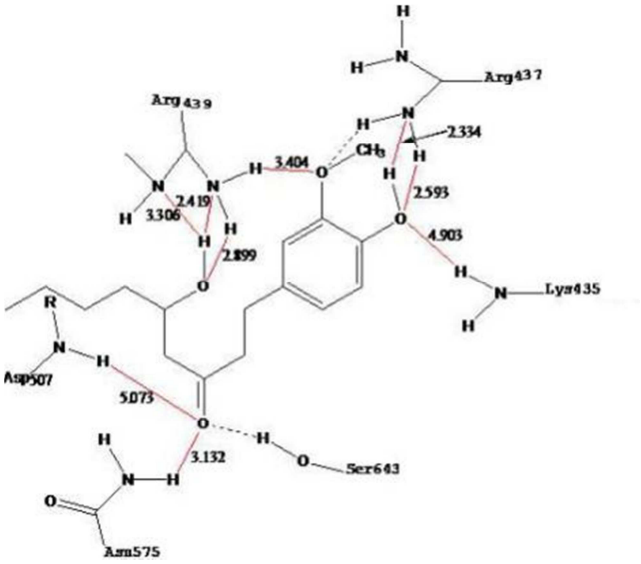

Figure 24. *Schematic representation of the binding of Compound 2 to the active site of the target enzyme.*

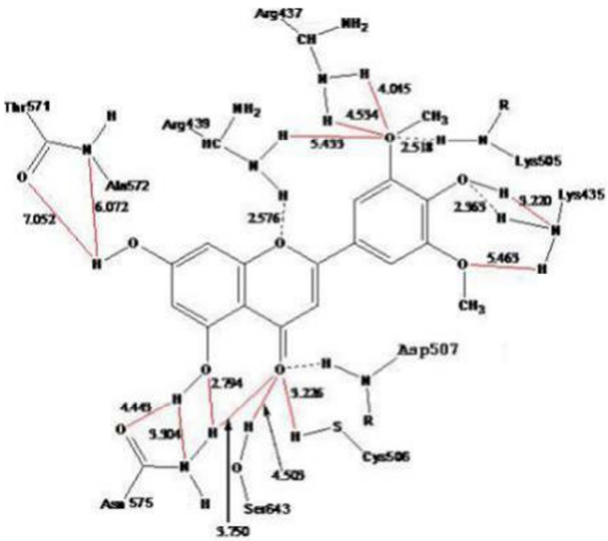

Figure 25. *Schematic representation of the binding of Compound 5 to the active site of the target enzyme.*

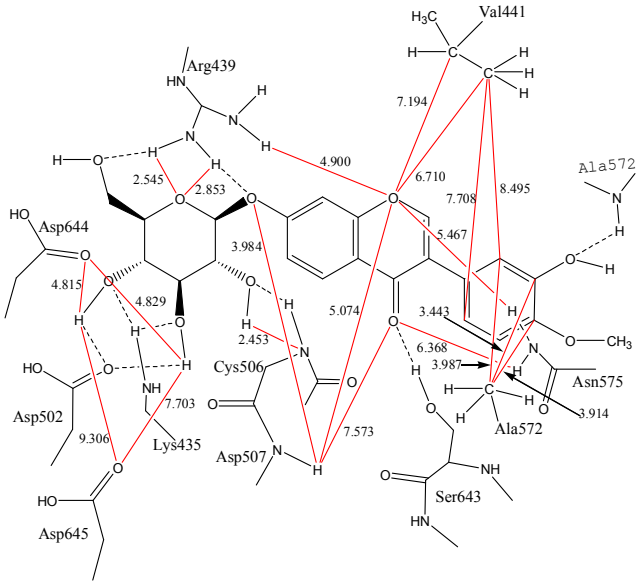

Figure 26. *Schematic representation of the binding of Compound 6 to the active site of the target enzyme.*

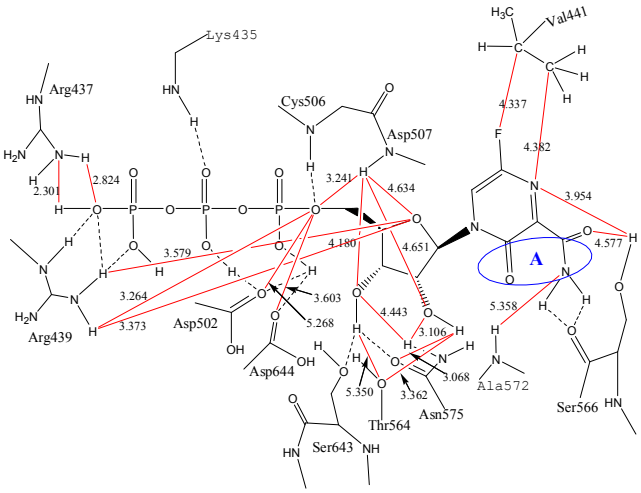

Figure 27. *Schematic representation of the binding of Compound 9 to the active site of the target enzyme.*

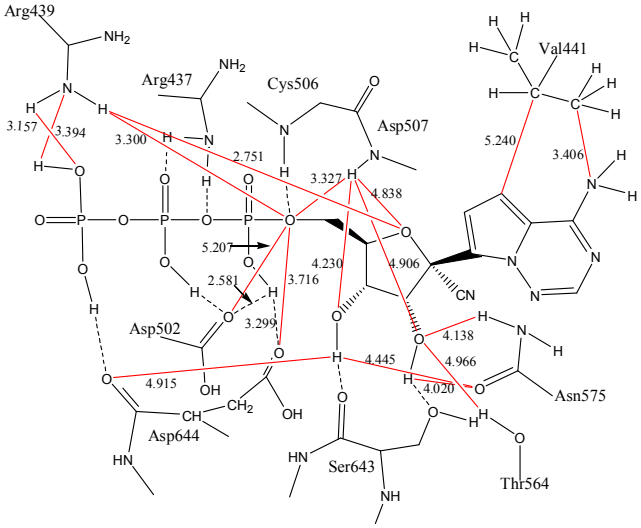

Figure 28. *Schematic representation of the binding of Compound 10 to the active site of the target enzyme.*

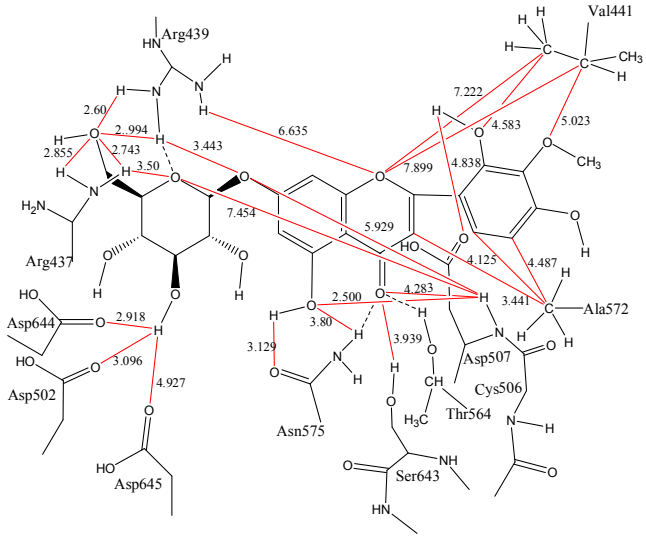

Figure 29. *Schematic representation of the binding of Compound 12 to the active site of the target enzyme.*

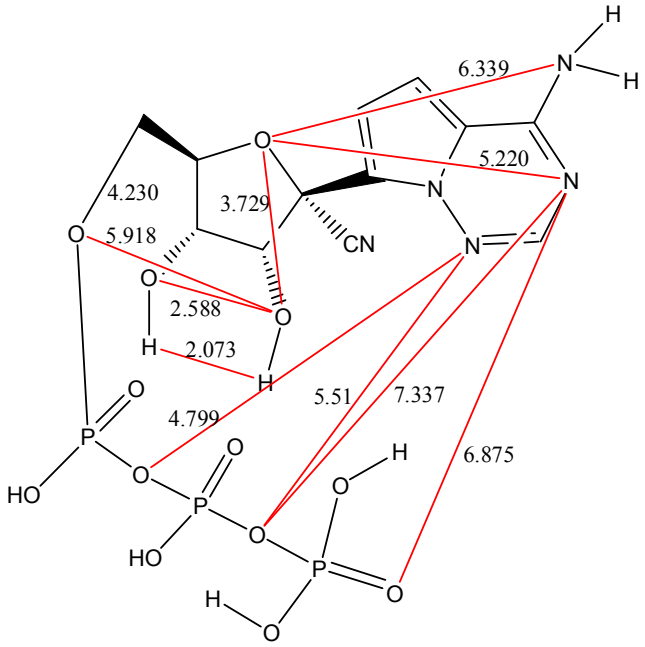

Figure 30. *Schematic representation of the binding of Compound 10 to the active site of the target enzyme.*

5. Analysis of Molecular Docking Results

The movement is relative, and the target enzyme is taken as the reference. The point where the raw nucleotide NTPs enters the active site of the target enzyme can be regarded as a relatively independent movement. In the model, amino acid Lys435, Ser433, Ala434, Lys322, Arg720, Asp717, His700, Gln699, Ser698, Cys697, Ala681, Lys682, Asp502, etc., surround the RNA template entry, and the distance between the hydroxyl hydrogen on Ser698 residues and Lys435 residues N atoms is 8.986 Å. The amino acids that bind to the template chain at the export end [8] are Tyr799, Tyr479, Phe478, Ser476, etc. The amino acids bound to the nascent RNA strand are Leu738, Ile731, Arg742, Ser745, etc. The

NTPs entry channel is relatively shallow, approximating the vertical RNA strand channel, Lys435 residue N-H and Asp502 Residual oxygen atoms form intramolecular hydrogen bonds (bond length 2.075Å). The distance between N atom and Asp502 residue oxygen atom is 2.873Å. Lys435 residue and Asp502 residue are the common edges of the above two channels, see Figure 7. If the RNA channel is compared to a cylinder, the NTPs entry channel is like a circular pore formed by cutting off a disc from the upper wall of the cylinder. The Lys505 residue on the surface of the pore extends approximately horizontally into the NTPs entry channel. It further encloses a small channel with Lys435, Arg437 residues and Tyr503, Pro504 skeletons. NTPs are likely to enter into the active site from this small channel. According to the diameter of the entry and the distribution of polar amino acids at the active site, it can be inferred that the sequence of the substrate NTPs passing through the entry is base, ribose and phosphate. In the model, Lys435, Arg437, Arg439, Asp502, Asn575, Asp644, Asp645 residues and 507 skeleton N-H around the active site of NTPs binding. The Arg439 residues almost point vertically to the channel cavity and are arranged in a deeper position of Arg437 residues. The three N-atom planes at the tail of Arg437 residues point obliquely to the Arg439 residues. The residues of Arg437 and Arg439 are very important for immobilizing the position of the substrate compound. The residues of Asp502 and Arg439 can also anchor the polar groups such as phosphate group of nucleoside substrate; The metal complexes of Asp502, Asp644 and Asp645 residues form the catalytic center of the target enzyme and play a key role in the synthesis of 3 '- 5' phosphate diester bond. Asp507 and Asn575 can form hydrogen bond interaction with newly entered nucleotide 2'-OH and participate in the discrimination and selection of ribose and deoxyribose by RNA polymerase. In addition, 564 seems to interact with 2 '- OH to form hydrogen bond [9, 12]. Ser643 may interact with 3'- OH at the end of primer chain and new NTPs. Val441 residue has the function of stabilizing the base at the +1 position of the template chain and ensuring the pairing between the newly entered NTP base and the base at the +1 position of the template chain. Therefore, when some nucleoside inhibitors bases are combined at the active site and play an inhibitory role, the base part should be toward Val441. The conformation of Favipiravir triphosphate, Remdesivir triphosphate and Acyclovir triphosphate is similar to "U" shape when they are combined with the active site of the target enzyme. The base part is toward Val441, but not far away along the opposite direction of Val441, there are Ala569, Lal572, Tyr573, Leu642, Ile473, Val379, Leu460, Tyr573 and Phe696 residues to form a hydrophobic cavity. Lal572 and Ala569 residues are at the entrance of the hydrophobic cavity. The oxygen atom of the carbonyl group is 5.277 Å away from the carbon atom of Lal572 residue, while the oxygen atom in the amide substituent is 7.227 Å away from Lal572 residue C. When the carbonyl group on the pyrazine ring extends outwards for about three chemical bonds, the hydrophobic cavity entrance can be reached, and the binding strength of the compound with the target enzyme can be enhanced by connecting the hydrophobic substituents such as cyclohexyl, cyclopentyl and benzene ring. When the triphosphate form of Remdesivir binds at the active site of the target enzyme, the base plane is parallel to the entrance of the hydrophobic pocket in the distance, -CN is 6.439Å from Lal572 residue C, and N atom is 8.658Å from Lal572 residue C. When Acyclovir triphosphate forms are combined at the active site of the target enzyme, the whole base part is toward Val441, but the five membered ring part of the base is closer to Val441, and the six membered ring part forms two intermolecular hydrogen bonds with Asn575 residue. If the base part is rotated 180°, the six membered ring part is toward Val441, which may be related to the steric hindrance of Acyclovir's ribose deficient part. The six membered sugar ring of compounds 6 and 12 occupy the five membered sugar ring position region of nucleoside inhibitors, but due to the hydrogen bond between the amino acids on the opposite side of Val441 and their mother nucleus, the binding region of the mother nucleus structure deviates from that of nucleoside inhibitors. The distance between one O atom in compound 6 and carbon atom in Val441 residue is 6.710 Å, while the distance between one O atom in compound 12 and carbon atom in Val441 residue is 7.222 Å, and the distance between three carbon atoms in compound 6 and carbon atom in Ala572 residue is 5.366 Å. In compound 12, the distance between the 3-carbon atom and Ala572 carbon atom is 3.441 Å, and the C-ring part is close to the hydrophobic cavity. In compound 6, the distance between the 2′, 3′, 4′ carbon atom and Ala572 carbon atom is 3.778 Å, 3.443 Å, 3.914 Å, respectively. In compound 12, the distance between the 5′, 6′ carbon atom and Ala572 carbon atom is 4.125 Å, 4.487 Å, respectively.

Based on the analysis of the binding mode of compounds 7, 18, 19, 20 and target enzyme structure, compounds 7 and 19 tend to enter NTPs channel first in ribose part than in base part, while compounds 18 and 20 tend to enter NTPs channel first in base part. Among them, the binding mode of compound 18 is in the highest agreement with the assumption of NTPs entry sequence made by the author. The base part of compound 18 is oriented to Val441, and the N atom on the amino group is 5.356Å away from the C atom of Val 441 residue. There is no N atom in the five membered ring, which is 5.244Å away from C atom of Val441 residue. Due to the interaction between the amino acid on the opposite side of Val441 and the base ring, the base part of compound 18 appears to be far away from the Val441 residue to some extent. The author thinks that the free energy (-6.3kal/mol) released by the binding site of compound 18 to the target enzyme is used as the standard for the evaluation of compound inhibition, and the result is more accurate than that (-5.9kal/mol) of compound 7. Compounds 3, 5 and 4 enter the NTPs channel in the opposite order. Compounds 4 tend to enter the C ring first.

In the binding mode of compound 16 with the active center of the target enzyme, the distance between the carbon atom of the para and inter position on the benzene ring and the carbon atom of Val441 residue is 3.630Å and 3.504Å. This shows that the benzene ring part is very close to the Val441 residue, which is likely to produce steric hindrance effect with the + 1

base of template chain, resulting in the change of current binding state of compound 16. Therefore, the inhibition effect of compound 16 on target enzyme should be treated carefully. Compounds 1 and 7 occupy almost the whole NTPs channel, and pyrrolidine part forms hydrogen bond with 435 and 502 residues at the entrance of NTPs channel. The dicyclo [2,2,2] octane part enters the intermediate region between Val441 residue and Ala572 residue, the nearest distance to CH3 atom of Val441 residue is 5.720 Å, and the nearest distance to carbon atom of Ala572 residue is 5.329 Å. The hydrogen atom on the carboxyl group and its connected oxygen atom form hydrogen bond interaction with the hydrogen atom on the skeleton carbonyl oxygen atom and the hydroxyl group of Ser643 respectively.

In summary, novel coronavirus RNA polymerase is strongly inhibited by compounds 4, 5, 6, 9, 10, and 17 in the 27 compounds reported in this report. Compound 16 may be a strong inhibitor of RNA polymerase. Compound 1, 3, 8, 11, 13, 14, 19, 20, 21, 22, 24, 27 are weak inhibitors of RNA polymerase, compound 2, 23, 25, 26 may be weaker. Flavonoid compounds have good inhibitory activity against RNA polymerase and are widely found in fruits, vegetables and some Chinese medicinal materials, with good safety. Therefore, they should be included in the novel coronavirus inhibitory activity test range. There are hydrophilic amino acids in the active sites of NTPs, such as Arg437 and 439, etc. enhancing the binding with hydrophilic amino acids can enhance the binding between compounds and enzymes, such as flavonoids, curcumin and gingerol, which enhance the binding ability with the active sites of NTPs in the target enzyme structure after they are linked to the sugar ring. Binding of the 5'- hydroxy group to the 3-phosphate group also enhances the binding ability to the target enzyme active site. The hydrophobic pocket surrounded by Lal572, Leu642, Val379 and other amino acid residues can be used. When the hydrophobic group of the inhibitor extends into the hydrophobic pocket, the binding ability of the inhibitor and the enzyme can be increased, which may make the activity of the inhibitor stronger.

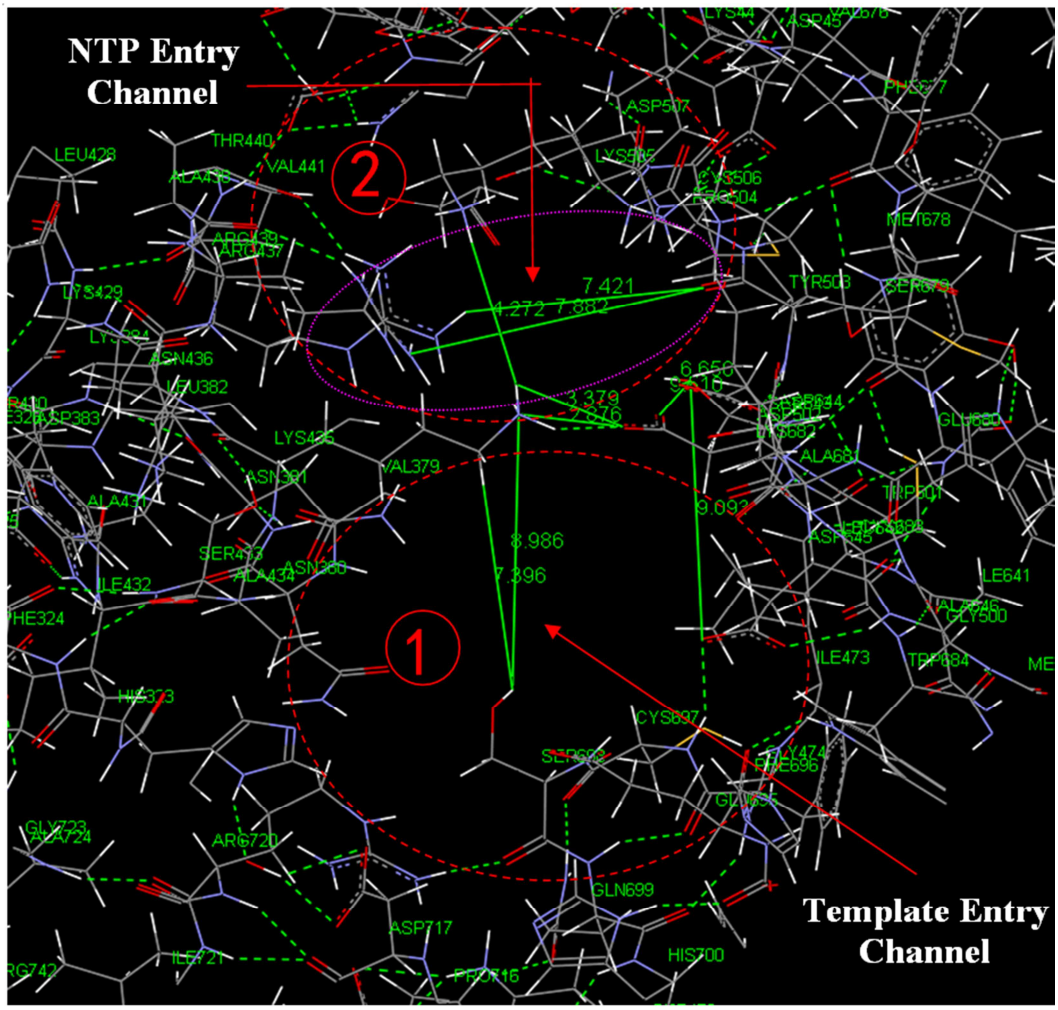

Figure 31. *Screenshots of RNA template chain channel entry and NTPs channel entry.*

6. Summary

Novel coronavirus RNA polymerase is a relatively reliable target for antiviral action. The author used the homology modeling method and took SARS RNA polymerase 6NUR as the template to construct the novel coronavirus RNA polymerase 3D structure model and found that some

traditional Chinese medicine chemical components can be competitive combined with NTPs at the active site of the target enzyme. The binding strength of some of the flavonoid compounds on the novel coronavirus RNA polymerase active site is similar to that of Remdesivir triphosphate and Favipiravir triphosphate, so the flavonoid compounds may be highly active anti-coronavirus active ingredients. And chemical components such as gingerol metabolites and shikonin with relatively weak binding effect may be weakly active anti-coronavirus components. According to the research results, the author speculated that flavonoid compounds such as chrysin, apigenin, luteolin, kaempferol, quercetin, baicalein, wogonin, scutellarin, galangin, eupatilin, genkwanin, jaceosidin, lysionotin, eupatorin, 4'-methoxy-5,7,3' -trihydroxyflavone, cosmosiin, galuteolin, chrysin glycosides, genistein, calycosin, ononin, dihydroquercetin, Naringenin, 5,7,4 '-trihydroxy-8-methyldihydroflavone, 4 '-methoxy -5,7,3' -trihydroxydihydroflavone and components such as coumarin, anthranol and flavonoid with specific substitution could inhibit novel coronavirus RNA polymerase, and all could play an antiviral effect. The author believes that ginger decoction (45g ginger + 40g scallion + brown sugar 25g) plus 30g astragalus and (or) 15g ephedra (or other traditional Chinese medicine containing flavonoids) is a powerful drug against novel coronavirus infection.

During the evolution of RNA virus, its RNA polymerase is very conservative, especially the evolution of functional amino acids is very slow. The three-dimensional structure of HCV RNA polymerase NS5B is similar to that of novel coronavirus [9, 11, 13], and the spatial structure of NTPs binding active site is basically the same. Flavonoid compounds can be combined with novel coronavirus RNA polymerase NTPs binding active site and play the role of inhibiting RNA synthesis, then flavonoid compounds should also be combined with hepatitis C virus RNA polymerase NTPs binding active site and play the role of anti-hepatitis c virus, this is the inevitable reasoning. It has been proved that many flavonoids target NS5B and have anti HCV effect [14-20]. For example, in the cell level test, the EC50 of apigenin against HCV is 7.9 μm, the EC50 of luteolin is 4.7 μm. The EC50 of compound 28 (Figure 8A) is 5 μm, and that of compound 29 (Figure 8b) is 0.0147 μm. These experimental data can also be regarded as indirect support for our research results. The *Daily Mail* reported on April 3 that a 99-year-old man in the United Kingdom had succeeded in fighting new coronavirus without taking any prescribed medication, and that the "secret ingredient" was marmalade and biscuits, which are rich in flavonoids. If the fact of news report is true, it may be another proof of the author's research results. In addition, the *Global Times* recently reported that figures have been instrumental in the fight against epidemics in Tunisia and are believed to have miraculous medicinal properties against new coronaviruses, while figures are also rich in flavonoids, consistent with the author's findings.

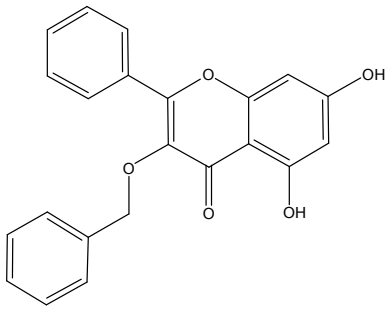

Figure 32. *Compound 28.*

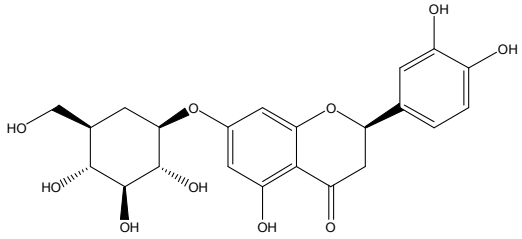

Figure 33. *Compound 29.*

In many cases, traditional Chinese medicine and modern medicine describe the nature of the same disease in the human body with different languages and the object is the same. As for the Chinese medicine prescription that novel Coronavirus infection treatment relies on, traditional Chinese medicine is also a realistic substance that contains a variety of natural compounds. The author believes that some traditional Chinese medicine components represented by flavonoids can well bind to the active site of NTPs in the three-dimensional structure of target enzyme, thus interfering the biological function of target enzyme and playing the role of fighting against coronavirus. According to the results of this experiment, if the patient was infected with novel Coronavirus, more vegetables and fruits rich in flavonoids should be added into the diet, which could play a positive role in the treatment of the patient. Effective treatment of infected people with antiviral drugs, coupled with cutting off the transmission of the novel coronavirus, may be fundamental to controlling the virus' ravages. We hope that our research and ideas will attract the attention of researchers at home and abroad, and that capable researchers will experiment further to obtain real data to verify the correctness or errors of our views and provide real and valuable reference for the global research and development of novel coronavirus drug. It will be a valuable reference to contribute to the early defeat of the novel coronavirus epidemic. In addition, we also hope that we can obtain funding, assistance and collaboration from relevant organizations to conduct relevant in-depth research.

Funding

1. Research Project of Hebei Provincial Administration of Traditional Chinese Medicine (2020180).
2. Research Project of Hebei Provincial Health Committee (20191055).

References

[1] Su Yanlei, Duan Xuhong, Xu Wencheng, *et al*. Screening of anti-2019-nCoV inhibitors with the target of RNA-dependent RNA polymerase [J]. *CHINESE ARCHIVES OF TRADITIONAL CHINESE MEDICINE*, 2020.3.15, Pre-proof, http://kns.cnki.net/kcms/detail/21.1546.R.20200313.1033.002.html

[2] Wu C, Liu Y, Yang Y, *et al*. Analysis of therapeutic targets for SARS-CoV-2 and discovery of potential drugs by computational methods, *Acta Pharmaceutica Sinica B*, https://doi.org/10.1016/j.apsb.2020.02.008.

[3] A. A. Elfiky. Ribavirin, Remdesivir, Sofosbuvir, Galidesivir, andTenofovir against SARS-CoV-2 RNA dependent RNA polymerase (RdRp): A moleculardocking study, *Life Sciences* (2020), https://doi.org/10.1016/j.lfs.2020.117592

[4] Muhammad Usman Mirza, Matheus Froeyen. Structural elucidation of SARS-CoV-2 vital proteins: Computational methods reveal potential drug candidates against main protease, Nsp12 polymerase and Nsp13 Helicase [J]. *Journal of Pharmaceutical Analysis* (2020), doi: https://doi.org/10.1016/j.jpha.2020.04.008

[5] Ashleigh Shannon, Nhung Thi Tuyet Le, Barbara Selisko, *et al*. Remdesivir and SARS-CoV-2: structural requirements at both nsp12 RdRp and Exonuclease [J]. Antiviral Research, 2020, https://doi.org/10.1016/j.antiviral.2020.104793Get rights and content

[6] Calvin J. Gordon, Egor P. Tchesnokov, Emma Woolner, *et al*. Remdesivir is a direct-acting antiviral that inhibits RNA-dependent RNA polymerase from severeacute respiratory syndrome coronavirus 2 with high potency [J]. JBC Papers in Press, Published on April 15, 2020 as Manuscript RA120.013679, The latest version is athttps://www.jbc.org/cgi/doi/10.1074/jbc.RA120.013679

[7] Abdo A. Elfiky. SARS-CoV-2 RNA dependent RNA polymerase (RdRp) targeting: an in silico Perspective, JOURNAL OF BIOMOLECULAR STRUCTURE AND DYNAMICS, https://doi.org/10.1080/07391102.2020.1761882

[8] Wanchao Yin, Chunyou Mao, Xiaodong Luan, *et al*. Structural basis for inhibition of the RNA-dependent RNA polymerase from SARS-CoV-2 by remdesivir, *Science,* 10.1126/science.abc1560 (2020).

[9] Yan Gao, Liming Yan, Yucen Huang. Structure of the RNA-dependent RNA polymerase from COVID-19 virus [J]. *Science*10.1126/science.abb7498 (2020).

[10] Yan Gao, Liming Yan, Yucen Huang, et al. Structural basis for inhibition of the RNA-dependent RNA polymerase from SARS-CoV-2 by remdesivir, *Science* 10.1126/science.abc1560 (2020).

[11] Yan Gao, Liming Yan, Yucen Huang, *et al*. Structure of RNA-dependent RNA polymerase from 2019-nCoV, a majorantiviral drug target, bioRxiv preprint doi: https://doi.org/10.1101/2020.03.16. 993386.

[12] Robert N. Kirchdoerfer, Andrew B. Ward. Structure of the SARS-CoV nsp12 polymerase bound to nsp7 and nsp8 co-factors [J]. NATURE COMMUNICATIONS, 2019.

[13] Luigi Buonaguro, Maria Tagliamonte, Maria Lina Tornesello, *et al*. SARS-CoV-2 RNA polymerase as target for antiviral therapy [J]. *Journal of Translational Medicine*, 2020, 18: 185, https://doi.org/10.1186/s12967-020-02355-3.

[14] Neerja Kaushik-Basu, Alain Bopda-Waffo, Tanaji T. Talele, *et al*. Identification and characterization of coumestansas novel HCV NS5B polymerase inhibitors [J]. Nucleic Acids Research, 2008, 36 (5): 1482–1496.

[15] Liu Ning. Research on anti HCV activity of flavanoid compounds [D]. Kunming university of science and technology, 2014.

[16] Zhong Jindong. Studies on the Chemical Constituents and Bioactivities of Two Medicinal Plants [D]. Kunming university of science and technology, 2013.

[17] Mingming Liu, Design, synthesis and anti-HCV activity of small molecules based on diketonic acid structures [D]. Fudan University, 2012.

[18] Dongwei Zhong, Mingming Liu, Yang Cao 1, et al. Discovery of Metal Ions ChelatorQuercetin Derivatives withPotent Anti-HCV Activities [J]. *Molecules* 2015, *20*, 6978-6999.

[19] Abdelhakim Ahmed-Belkacem, Jean-Francois Guichou, Rozenn Brillet, et al. Inhibition of RNA binding to hepatitis C virusRNA-dependent RNA polymerase: a new mechanismfor antiviral intervention [J]. *Nucleic Acids Research, 2014, 42 (14): 9399–9409.*

[20] Ana Carolina Gomes Jardim, Jacqueline Farinha Shimizu, Paula Rahal and MarkHarris. Plant-derived antivirals against hepatitis cvirus infection [J]. *Virology Journal*, 2018, 15 (34): 1-13.